LOW COST NUMERICAL MODELING OF MATERIAL JETTING-BASED ADDITIVE MANURACTURING

Chad A. Hume, David W. Rosen*

George W. Woodruff School of Mechanical Engineering
Georgia Institute of Technology
Atlanta, GA 30332

*Corresponding author. Email: david.rosen@me.gatech.edu

Abstract

Material jetting-based additive manufacturing is a promising manufacturing approach with increasing interest in mesoscale applications such as microfluidics, membranes, and microelectronics. At these size scales, significant edge deformation is observed limiting the resolvable feature size. Currently, predicting and controlling such deformations would require extensive experimentation or computationally prohibitive simulations. The objective of this work is to develop a computationally low cost material jetting model that enables the simulation and prediction of mesoscale feature fabrication. To this end, a quasi-static boundary-based method is proposed and demonstrated as a simplified and accurate means of predicting the line-by-line, layer-by-layer feature development. The method is validated through comparison with the known analytical solution for a single droplet; then the method's application to AM is demonstrated through modeling of representative mesoscale features. The benefits and limitations of each are discussed.

Introduction

Additive manufacturing (AM) has been widely adopted as a rapid and highly flexible class of fabrication techniques. One of the key advantages cited for the adoption of AM is the geometric freedom to produce parts of near infinite complexity, fueling design innovations in many industries. Like its more traditional manufacturing counterparts, AM is not without its manufacturing constraints. These constraints vary between different AM processes, requiring a detailed understanding of the effects of geometric and process parameters for each specific process. Of particular interest in this work is the material jetting process.

Material jetting-based (MJ) processes are a promising approach for AM, benefiting from the significant process development achieved by commercial 2D inkjet printing. To fabricate parts, banks of print heads selectively eject streams of droplets onto a build platform positioned below. These droplets then coalesce to form deposited lines, and overlapping lines form a final layer. Subsequent layers are deposited in the same fashion, one of top of the other, to form a 3D geometry. MJ machines are among the highest resolution AM processes, with the added benefit of scalability in both size and speed. Ejected droplets can be melted material, suspensions, or photopolymer liquids; no other AM technology offers as much material flexibility as MJ nor the ability to deposit different materials on a pixel-by-pixel basis.

With these advantages material jetting-based fabrication has attracted significant research and development efforts as a novel fabrication technique with particular focus on mesoscale applications. Open areas of interest include printed electronics [1], microfluidics [2], and "4D" printing [3]. As these new applications develop, MJ systems are increasingly pushing into new frontiers of size, complexity, and functionality, testing the limits of current machines. In fact, characterization of existing machines has shown significant geometric deformities at the mesoscale, such as sloped walls and rounded corners [4,5]. It is therefore critical to develop a strong understanding of underlying physical processes along with models capable of accurately and efficiently predicting the fabricated geometry.

Toward that end, the objective of this work is to develop a computationally low cost material jetting model that enables the simulation and prediction of mesoscale feature fabrication. A quasi-static boundary-based method is proposed and demonstrated as a simplified and accurate means of predicting the line-by-line, layer-by-layer feature development. In the next section, relevant literature is reviewed along with a discussion of the existing limitations. Next, the underlying theory, assumptions and method are presented. The method is validated through comparison with the known analytical solution for a single droplet, before demonstrating the fuller capability modeling mesoscale feature fabrication.

Literature Review

The long history of inkjet-based printing provides a significant volume of literature on the modeling of droplet impingement. Both analytical and numerical studies abound, covering single droplet impingement, droplet coalescence, and line formation under various process conditions. For a general review of this literature, the reader is referred to work by Derby [6]. While certainly requisite for understanding the deposition process, the existing inkjet literature suffers from two major short comings relative to AM processes. First, these works assume a uniform flat surface. This is clearly insufficient for the AM process. Only for the first passes of the first layer will deposition occur on a uniform, flat surface. Subsequent passes and layers are deposited on previously deposited lines or layers, which at a minimum will be uneven at the edges. Second, many of the traditional computation fluid dynamic (CFD) approaches utilized, such as volume-of-fluid, level-set, and phase-field, are extremely computationally demanding. This severely limits the number of droplets that can be incorporated, with four droplets being the most observed in existing literature [7]. To address this computational burden, Zhou developed a Lattice Boltzmann based numerical model to explore droplet interface dynamics and the interactions of multiple droplets in a layer [8]. The benefit of his approach is the ability to parallelize the simulation such that it can be run on a larger number of computer threads to boost simulation efficiency. While promising, the Lattice Boltzmann approach is still very computationally demanding, requiring a high performance computing cluster to scale up, and has only been demonstrated for up to nine droplets.

In terms of AM specific process modeling, a few works have sought to develop closed-loop control methods for the MJ process, utilizing droplet-level deposition models in their feedback loop. Cohen and Lipson estimated the deposition field height by assuming each droplet can be approximated as a spherical cap, where the resulting height is simply a linear addition of the overlapping regions [9]. This height map is then used within the feedback loop of their "greedy geometric feedback" control algorithm along with real-time measurements. In several works, Mishra et al. developed a model based feedback control algorithm using an empirical

height change model for the deposition of one droplet next to its neighbors [10], [11]. Given a uniform printing grid, it was assumed that the height of a given point on that grid is affected by the center droplet, side droplets, and corner droplets. The height change is then the resulting summation of all the contributions of these droplets. The main limitation of these works is the limited ability to incorporate the effects from droplet-level material flow into a global process model, such that feature errors like sloped walls and rounded corners can be captured.

Quasi-static Boundary-based Method: Theory and Implementation

Theory

The present approach is based on the work of Thompson et al., which developed a reduced dimensional model to predict the morphology of inkjet printed lines deposited on a flat surface [12]. This was accomplished by approximating the complex initial dynamics with a simple droplet spreading factor to define the post impingement contact line, then solving the subsequent problem using a quasi-static spreading law.

When a jetted droplet impacts the substrate surface, its shape undergoes a complex evolution as it transitions from a spherical shape in flight to its final equilibrium shape, as shown in Figure 1. A number of physical parameters affect this evolution and the relative significance of inertial forces, capillary forces, and gravitational forces. These parameters include droplet size (D_0), deposition velocity (U), fluid density (ρ), viscosity (μ), surface tension (σ), and material-surface interaction like contact angle (θ).

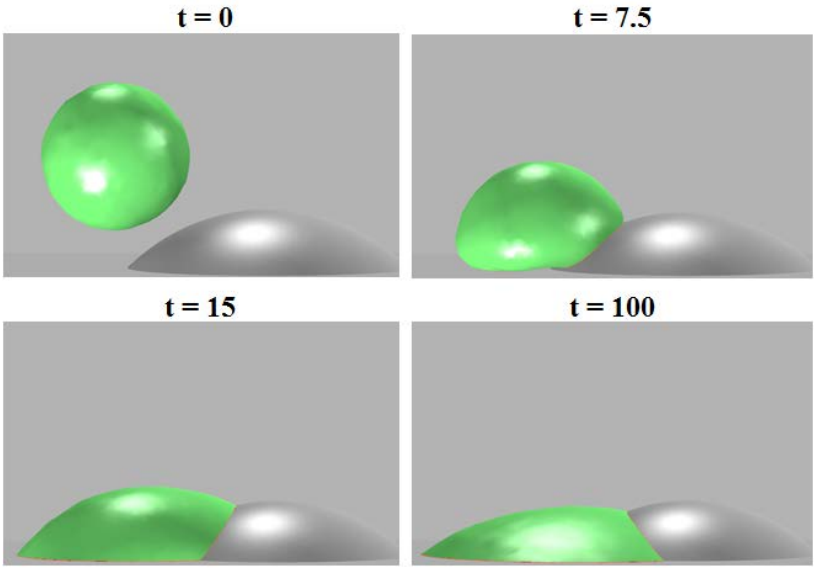

Figure 1: Evolution of a 40μm diameter droplet impacting onto a cured droplet (time in μs)

For the deposition of interest to this work, the shape evolution is generally divided into three phases. The initial impact phase is dominated by kinetic behavior determined by the impact velocity. The expansion of the droplet is balanced by both surface tension and viscosity. During the second phase, depending on the extent of initial expansion and fluid surface interactions, the droplet could relax back from expansion or could remain stationary experiencing contact angle hysteresis. For the fluids of interest to material jetting, this phase is generally well damped,

showing minimum or no oscillation. Finally, in the last phase, capillary forces dominate as the fluid spreads to its final sessile shape.

The relative time scales for each of these phases can be approximated using the following equations:

$$t_{spread} \approx \frac{D_0}{U} \; ; \; t_{osc} \approx \sqrt{\frac{\rho {D_0}^3}{\sigma}} \; ; \; t_{visc} \approx \frac{\rho {D_0}^2}{\mu} \tag{1}$$

Using Equation 1 along with representative values of MJ process parameters the time scales for the three phases are listed in Table 1. As a rough order of magnitude estimate, the transition from the relaxation phase to the final capillary phase is taken as half the viscous time period.

Table 1: Time scales of droplet spreading

ρ (kg/m^3)	μ (Pa·s)	σ (N/m)	D_0 (µm)	U (m/s)
1000	0.010	0.025	40	4
t_{spread} (µs)	t_{osc} (µs)	t_{visc} (µs)	t_{relax} (µs)	t_{dep} (µs)
10	50	160	80	125

To put these time scales into perspective we'll compare the printing deposition interval, t_{dep} (the time between subsequent drops). We estimate the ejection rate for an Objet machine to be ~8 kHz, based on speed of the printhead and known resolution, giving a deposition interval of 125 µs. We can see that the initial droplet spreading and oscillation is much faster than the droplet deposition, meaning that the fluid bead fully reaches the capillary stage before subsequent deposition. This is a great benefit towards simplifying our fluid modeling. In the capillary stage for a fluid with low Ohnesorge number, the bead evolution can be considered quasi-static such that the fluid surface can be determined based on the contact line boundary and the Young-Laplace equation [12]. Therefore, with a reasonable prediction of the droplet footprint after the spreading phase, the final fluid surface can be determined with reasonable accuracy without having to solve the full fluid problem as shown next.

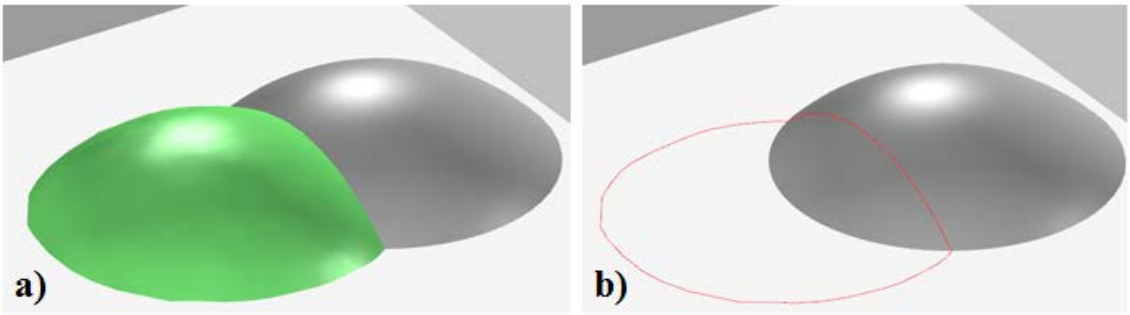

Figure 2: a) Droplet in quasi-static state, b) fluid substrate contact line

Consider a fluid wetting a surface in a quasi-static or equilibrium state like the one shown in Figure 2a. Assuming gravitational forces are negligible, *Bond* << 1 as is the case in this work, the pressure drop across the liquid-gas interface is described by the Young-Laplace equation:

$$\Delta p = \sigma \left(\frac{1}{R_1} + \frac{1}{R_2} \right) \tag{2}$$

where Δp is the pressure drop across the fluid interface, σ is the surface tension, and R_1 and R_2 are the principal radii of curvature.

The Young-Laplace equation assumes that on the interface the only stress applied is from external pressure and the resulting pressure drop is balanced by the surface tension forces, determined by the product of the bulk surface tension parameter, σ, and the mean curvature $\left(\frac{1}{R_1} + \frac{1}{R_2} \right)$. Since the liquid is assumed to be in a quasi-static state, tangential stresses are assumed to be negligible.

Expressing Equation 2 in terms of Cartesian coordinates, where the height of the liquid interface is $z = h(x, y)$, yields the following equation:

$$\Delta p = -\sigma \, \nabla \cdot \frac{\nabla h}{\sqrt{1+|\nabla h|^2}}, (x, y) \in \Omega, \Gamma(x, y) = s(x, y) \tag{3}$$

where Ω is the wetted region, Γ is the contact line, and $s(x, y)$ is the height profile of the substrate.

Equation 3 is a second order nonlinear partial differential equation of the elliptic form and fully describes the fluid interface so long as $h(x, y)$ and $s(x, y)$ are unique for any point (x, y). Given a prescribed pressure drop and associated boundary conditions, Equation 3 can be solved to determine the fluid interface height; however, typically the associate pressure drop across the interface is not known *a priori*. Fortunately, since our deposited material has a known mass and is assumed incompressible, the volume of material is known. By adding a matching volume constraint, calculated using Equation 4, the pressure drop can be varied iteratively to solve for the interface height:

$$V = \int_{\Omega} (h(x, y) - s(x, y)) dx dy \tag{4}$$

It should be noted that solving nonlinear PDE's numerically is far from trivial and nearly impossible analytically for any complex domain. For this reason, many works seek to simplify to a linear form by adopting the thin film approximation shown in Equation 5, which drops the first derivative terms with the error vanishing as a function of the square of the slopes.

$$\Delta p = \sigma \nabla^2 h(x, y) = \sigma \left(h_{xx} + h_{yy} \right) \tag{5}$$

Equation 5 represents a second order linear partial differential equation of the elliptic form and is equivalent to the commonly seen Poisson equation. As such, solving for the resulting height field is much more manageable resulting in better stability and faster solutions so long as the resulting error is acceptable. The degree of this error will be tested later during validation.

Implementation

The above model is solved numerically using the finite element method implemented in MATLAB. The finite element method is a power tool whereby a geometric domain of interest is divided into a collection of subdomains over which approximate solutions to the governing equations are solved, and then assembled together to form a piecewise solution to the problem of interest. The benefits of such an approach are far reaching, but most important are the ability to represent complex geometric domains with simple subdomains (finite elements) and the ability to reduce the solution of governing equation over these domains to much more manageable systems of algebraic equations. There are several common finite element approaches. The MATLAB implementation utilizes the weighted-residual approach (also known as the Galerkin).

The method used consists of three steps described below and demonstrated by modeling a line consisting of five sequential droplets, deposited at the edge of a previous layer, shown in Figure 3.

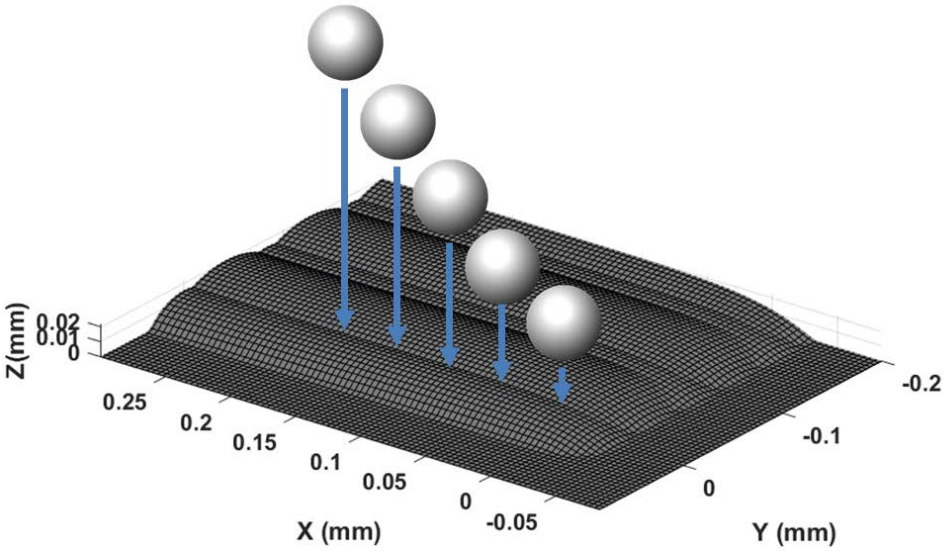

Figure 3: Line deposited at edge of previous layer

Step 1: Define the domain boundary

The first step towards defining the domain boundary is to estimate the contact line boundary of fluid in contact with the substrate. For each droplet, it is assumed that the fluid will flow outward from the deposition site, and the distance traveled can be modeled with a spreading law. For now, a simple spreading law is considered: distance traveled in each radial direction and over the surface is a constant value, where the constant is determined based on a single droplet spreading on a flat surface. A more sophisticated second spreading law could consider how the slope of the substrate at each deposition site would change the spread distance in each radial direction.

An example of the predicted spread for five sequential drops at the edge of an existing layer is shown in Figure 4.

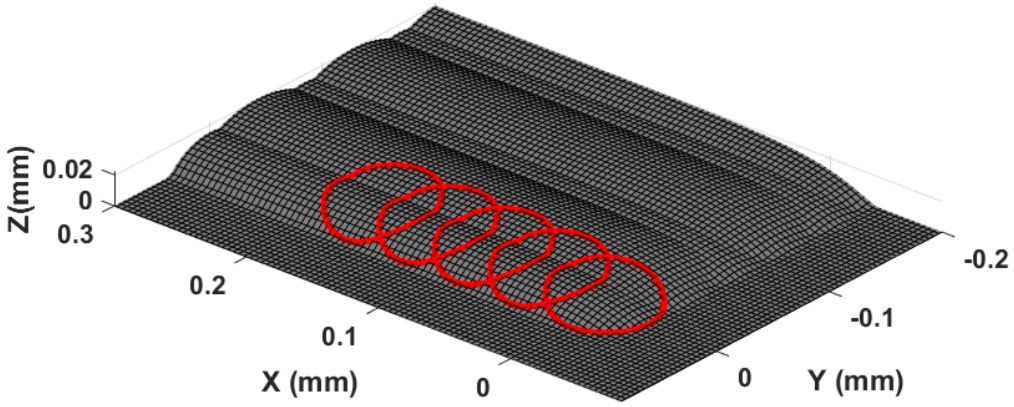

Figure 4: Predict droplet spread

Next, the droplet profiles are projected onto the *x-y* plane and the convex hull of the points is determined. The resulting represents the 2D domain boundary of the problem. On this boundary, a Dirichlet boundary condition is used, which specifies the value of the solution at the boundary of the domain. Since the domain boundary is the point where the fluid interface meets the substrate at the contact line, the associate boundary value at each point is simply the height of the surface at that point, which is set by using the substrate height from the previous layer and interpolating for any points between the grid spacing.

Step 2: Mesh the domain

With the domain boundary and associated boundary conditions set, the domain is now meshed with triangular elements. When meshing the domain, maximum element size and element order (linear or quadratic) is specified. These selections impact both solution accuracy and simulation time. The relative influence of these parameters is evaluated during validation below.

Step 3: Solve the PDE and Volume Constraint

With the boundary conditions set and the domain meshed, the fluid surface problem is solved using the finite element method implemented in MATLAB. As was previously stated, since the specific interface pressure difference is not known *a priori*, a volume constraint is used. This is implemented as a bounded search problem, to find the associated pressure difference to satisfy the volume constraint after the surface is solved. Thus, to begin the search, an initial pressure value is given and the PDE is solved over the finite element domain. The volume of the solution is calculated using the trapezoidal method, subtracting the volume of the substrate beneath the domain. The volume difference is then calculated and used to generate the next pressure value based on the gradient of the volume solutions. This is repeated iteratively until the volume constraint is met. Stopping criteria is set to a percent volume difference under 0.5. The solution of the example problem is shown in Figure 5.

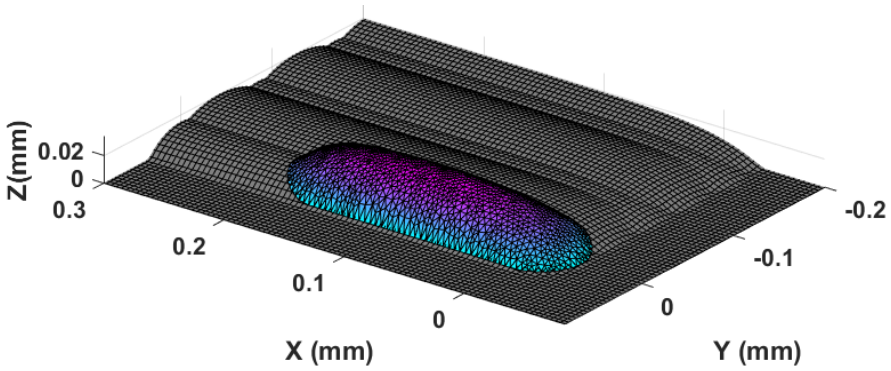

Figure 5: Solution for 3D fluid interface

Results and Discussion

Validation

To evaluate the boundary-based method's capacity to efficiently predict a deposited fluid surface, we compare the FEA simulation results for a single droplet on a flat surface with a spherical cap, shown in Figure 6, which is the known analytical solution to the Young-Laplace model for a micro-scale sessile drop. For this comparison, a 30pL droplet with a 45° static contact angle is used, resulting in a base radius of 35.2 µm and center height of 14.6 µm.

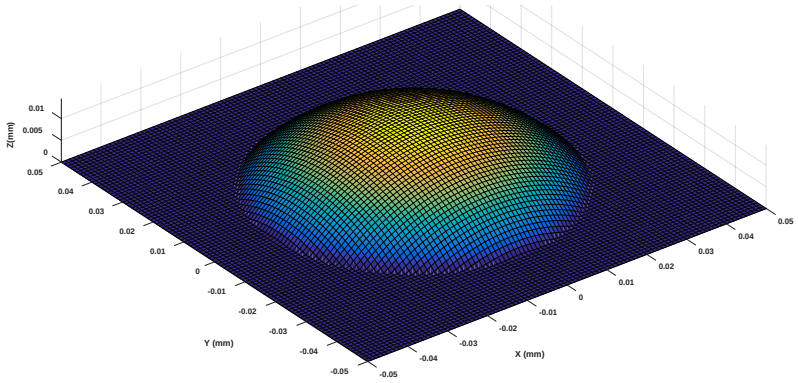

Figure 6: Spherical Cap

The numerical solution is calculated and evaluated for the mean absolute error throughout the domain and center height error compared with the spherical cap. The effect of mesh size/density and element order is evaluated, with results shown in Table 2. Overall, the numerical solution using the nonlinear formulation is quite accurate for both types of elements, as well as the coarsest mesh sizes, having a maximum average absolute error less than 0.2µm and maximum center height error less than 0.25µm. Comparing the quadratic elements with the linear elements reveals a significant increase in simulation time for only a minor improvement in terms of accuracy. The linear formulation boasts an additional reduction in simulation time, but has increased error. Both the nonlinear and linear formulations present orders of magnitude reduction in simulation time compared with a full 3D simulation, while still preserving acceptable accuracy. For comparison, the single droplet simulation shown in Figure 1 would need over 6 hours of simulation time using the level-set method in COMSOL.

As an additional validation, the method was run using parameters from the work of Lee and Son, who studied the deposition of up to four sequential droplets [7]. The boundary-based method showed good agreement with their work.

Table 2: Effects of mesh size and order on simulation time and accuracy

		Nonlinear Form 2nd Order Elements			**Nonlinear Form 1st Order Elements**			**Linear Form 1st Order Elements**		
***Elem max* (μm)**	***No. Elem***	Err_{avg} **(μm)**	Err_{cent} **(μm)**	$Time$ **(sec)**	Err_{avg} **(μm)**	Err_{cent} **(μm)**	$Time$ **(sec)**	Err_{avg} **(μm)**	Err_{cent} **(μm)**	$Time$ **(sec)**
10	136	0.082	0.104	19.01	0.177	0.230	8.78	0.273	1.012	0.99
5	504	0.102	0.175	19.23	0.114	0.209	8.33	0.305	0.945	1.19
2.5	2118	0.098	0.171	29.21	0.100	0.185	11.57	0.321	0.941	1.88

Modeling Mesoscale Features

Having validated the Quasi-static Boundary-based Method, feature fabrication is now investigated. The model parameters are based on the Objet Connex 260 printer specifications, which has a reported 600 dpi resolution in the x and y axes resulting in 42.3 μm droplet and line spacing. To achieve this resolution, the system requires four deposition passes and the nozzle spacing is such that during any single pass, fluid from two adjacent nozzles doesn't interact. For this study a 30pL droplet with a 45° static contact angle is used.

A 1x1mm square extrusion is modelled with a desired thickness of 0.2mm. This equates to a 25x25 droplet grid, 10 deposited layers, and a total of 6,250 droplet deposition sites. Overall, it took approximately 15 minutes to complete the simulation, averaging about 90 seconds per layer. Such a simulation would be unimaginable using any traditional CFD approach.

The final predicted geometry is shown in Figure 7.

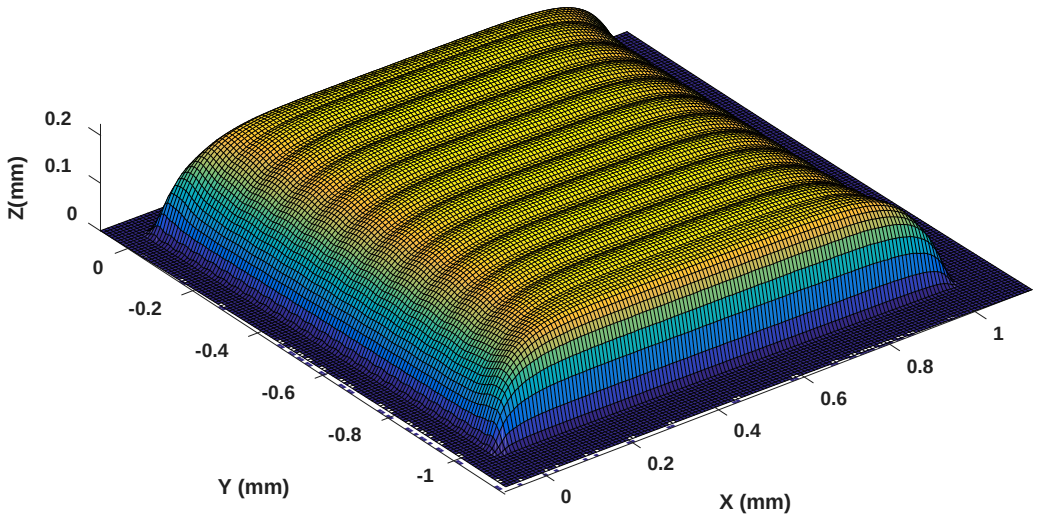

Figure 7: 1x1mm square after 10 layers

Figure 8 shows a side view of the simulated feature along with a feature fabricated using a Connex 260 machine. Qualitatively there is a good match between the boundary-based method and the fabricated part with its rounded corners and sloped walls. With greater details of the specific machine deposition parameters and fluid properties, this prediction would become increasingly accurate.

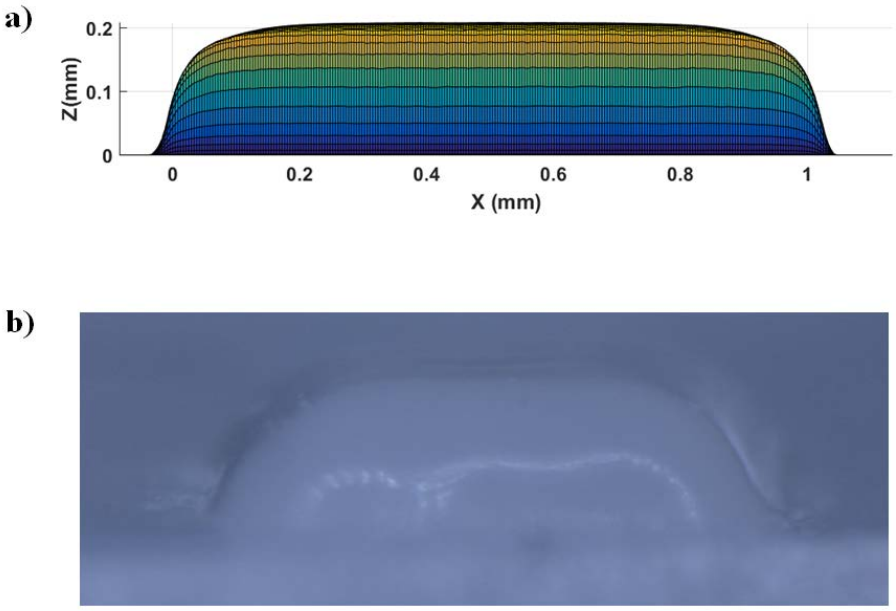

Figure 8: a) Side view of simulated feature, b) side view of fabricated feature

Conclusion

In this work, a quasi-static boundary-based approach is proposed to model the line-by-line, layer-by-layer shape evolution of the material jetting process. The method was validated through comparison with the exact solution for a hemispherical drop and the results of a high fidelity CFD simulation found in literature, showing very close results in both cases. The approach was then extended to simulate fabrication of a mesoscale square extrusion. The predicted feature shows rounded corners and sloped walls as a result of the MJ process, which is qualitatively verified by experimental characterization of a commercial machine. While preliminary in nature, the results presented above lay a strong foundation for the effectiveness of the proposed method to predict the MJ process. For future works, the initial droplet spreading will be investigated along with a deeper analysis of the computational efficiency of the proposed method.

References

[1] K. Yoshihiro, S. Hodges, B. S. Cook, C. Zhang, and G. D. Abowd, “Instant inkjet circuits: Lab-based Inkjet Printing to Support Rapid Prototyping of UbiComp Devices,” *Proc. 2013 ACM Int. Jt. Conf. Pervasive Ubiquitous Comput. - UbiComp ’13*, pp. 363–372, 2013.

[2] W. Su, B. S. Cook, Y. Fang, and M. M. Tentzeris, “Fully inkjet-printed microfluidics: a solution to low-cost rapid three-dimensional microfluidics fabrication with numerous electrical and sensing applications,” *Sci. Rep.*, vol. 6, no. 1, p. 35111, 2016.
[3] Z. Ding, C. Yuan, X. Peng, T. Wang, H. J. Qi, and M. L. Dunn, “Direct 4D printing via active composite materials,” *Sci. Adv.*, vol. 3, no. 4, p. e1602890, 2017.
[4] J. M. Lee, M. Zhang, and W. Y. Yeong, “Characterization and evaluation of 3D printed microfluidic chip for cell processing,” *Microfluid. Nanofluidics*, vol. 20, no. 1, p. 5, Jan. 2016.
[5] Y. L. Yap, C. Wang, S. L. Sing, V. Dikshit, W. Y. Yeong, and J. Wei, “Material jetting additive manufacturing: An experimental study using designed metrological benchmarks,” *Precis. Eng.*, vol. 50, pp. 275–285, 2017.
[6] B. Derby, “Inkjet Printing of Functional and Structural Materials: Fluid Property Requirements, Feature Stability, and Resolution,” *Annu. Rev. Mater. Res*, vol. 40, pp. 395–414, 2010.
[7] W. Lee and G. Son, “Numerical study of droplet impact and coalescence in a microline patterning process,” *Comput. Fluids*, vol. 42, no. 1, pp. 26–36, 2011.
[8] W. Zhou, “Interface Dynamics in Inkjet Deposition,” Georgia Institute of Technology, 2014.
[9] D. L. Cohen and H. Lipson, “Geometric feedback control of discrete-deposition SFF systems,” *Rapid Prototyp. J.*, vol. 16, no. December 2007, pp. 377–393, 2010.
[10] L. Lu, J. Zheng, and S. Mishra, “A Layer-To-Layer Model and Feedback Control of Ink-Jet 3-D Printing,” *IEEE/ASME Trans. Mechatronics*, vol. 20, no. 3, pp. 1056–1068, 2015.
[11] Y. Guo and S. Mishra, “A predictive control algorithm for layer-to-layer ink-jet 3D printing,” *Proc. Am. Control Conf.*, vol. 2016–July, pp. 833–838, 2016.
[12] A. B. Thompson, C. R. Tipton, A. Juel, A. L. Hazel, and M. Dowling, “Sequential deposition of overlapping droplets to form a liquid line,” *J. Fluid Mech.*, vol. 761, pp. 261–281, 2014.